Short-latency ocular following responses to motion stimuli are strongly affected by temporal modulations of the visual content during the initial fixation period

Boris M. Sheliga Laboratory of Sensorimotor Research, National Eye Institute, National Institutes of Health, Bethesda, MD, USA

Christian Quaia Laboratory of Sensorimotor Research, National Eye Institute, National Institutes of Health, Bethesda, MD, USA

Edmond J. FitzGibbon Laboratory of Sensorimotor Research, National Eye Institute, National Institutes of Health, Bethesda, MD, USA

Bruce G. Cumming Laboratory of Sensorimotor Research, National Eye Institute, National Institutes of Health, Bethesda, MD, USA

Neuronal and psychophysical responses to a visual stimulus are known to depend on the preceding history of visual stimulation, but the effect of stimulation history on reflexive eye movements has received less attention. Here, we quantify these effects using short-latency ocular following responses (OFRs), a valuable tool for studying early motion processing. We recorded, in human subjects, the horizontal OFRs induced by drifting vertical 1D pink noise. The stimulus was preceded by 600 to 1000 ms of maintained fixation (on a visible cross), and we explored the effect of different stimuli ("fixation patterns") presented during the fixation period. We found that any temporal modulation present during the fixation period reduced the magnitude of the subsequent OFRs. Even changes in the overall luminance during the fixation period induced significant suppression. The magnitude of the effect was a function of both spatial and temporal structure of the fixation pattern. Suppression that was selective for both relative orientation and relative spatial frequency accounted for a considerable fraction of total suppression. Finally, changes in stimulus temporal structure alone (i.e. "flicker" versus "transparent motion") led to changes in the spatial frequency tuning of suppression. In the time domain, the suppression developed quickly: 100 ms of temporal modulation in the fixation pattern produced up to 80% of maximal suppression. Recovery from suppression was instead more gradual, taking up to several seconds. By presenting transparent motion during the fixation period, with opposite motion signals having different spatial frequency content, we also discovered a direction-selective component of suppression, which depended on both the frequency and the direction of the moving stimulus.

Introduction

Neuronal and psychophysical responses to visual stimuli strongly depend on recent stimulus history, and numerous electrophysiological and perceptual studies document effects of prolonged (seconds or minutes) as well as brief (fractions of a second) adaptation of different attributes of visual stimuli, such as contrast, orientation, position, spatial frequency, direction of motion, etc. In the visual motion domain, a great deal of work has been directed toward better understanding of mechanisms underlying the motion after effect (MAE; for review, see Burr & Thompson, 2011; Mather, Pavan, Campana, & Casco, 2008). Studies using short-latency reflexive eye movements—ocular following responses (OFRs; Gellman, Carl, & Miles, 1990; Miles, Kawano, & Optican, 1986)—also made contributions in this line of research. For instance,

Citation: Sheliga, B. M., Quaia, C., FitzGibbon, E. J., & Cumming, B. G. (2021). Short-latency ocular following responses to motion stimuli are strongly affected by temporal modulations of the visual content during the initial fixation period. *Journal of Vision*, *21*(5):8, 1–18, https://doi.org/10.1167/jov.21.5.8.

https://doi.org/10.1167/jov.21.5.8 Received October 15, 2020; published May 10, 2021 ISSN 1534-7362

Taki, Miura, Tabata, Hisa, and Kawano (2009) used random-dot stimuli and showed that same direction OFRs (adapting versus test stimuli) were diminished, whereas opposite direction OFRs were at times enhanced. A significant advantage of studying the OFR is that these eye movement responses appear closely linked with neuronal activity at early stages of visual processing (V1, MT, and MST; for review, see Masson & Perrinet, 2012; Miles, 1998; Miles & Sheliga, 2010).

In a series of experiments described herein, we used the OFRs to study how different types of visual stimulation—achieved by presenting a variety of patterns during the initial fixation period (lasting for up to 1 second)—influenced the OFRs to motion stimuli that followed. Experiment 1 compared effects of static and dynamic fixation patterns. In Experiment 2, we used "flicker" and "transparent-motion" band-pass noise stimuli to measure the spatial frequency (SF) tuning of adaptation effects. Experiment 3 used transparent-motion, with different SF content for the two (opposite) directions of motion, revealing the impact of competition between different SFs during the fixation period. Finally, Experiment 4 addressed the time course of the adaptation effects.

Preliminary results of this study were presented in abstract form elsewhere (Sheliga, Quaia, FitzGibbon, & Cumming, 2017; Sheliga, Quaia, FitzGibbon, & Cumming, 2018).

Experiment 1

Materials and methods

Many of the techniques were similar to those used in this laboratory in the past (e.g. Sheliga, Chen, FitzGibbon, & Miles, 2005). Experimental protocols were approved by the institutional review committee concerned with the use of human subjects. Our research was carried out in accordance with the Code of Ethics of the World Medical Association (Declaration of Helsinki), and informed consent was obtained for experimentation with human subjects.

Subjects

Three subjects took part in this study: two were authors (BMS and EJF) and the third was a paid volunteer (TH) naïve as to the purpose of the experiments. All subjects had normal or corrected-to-normal vision. Viewing was binocular.

Eye movement recording

The horizontal and vertical positions of the right eye were recorded with an electromagnetic induction technique (Robinson, 1963). A scleral search coil embedded in a silastin ring (Collewijn, Van Der Mark, & Jansen, 1975) was placed in the right eye under topical anesthesia, as described by Yang, FitzGibbon, and Miles (2003).

Visual display and stimuli

Dichoptic stimuli were presented using a Wheatstone mirror stereoscope. In a darkened room, each eye saw a computer monitor (HP p1230 21 inch CRT) through a 45 degree mirror, creating a binocular image 521 mm straight ahead from the eyes' corneal vertices, which was also the optical distance to the images on the two monitor screens. Each monitor was driven by an independent personal computer (PC; Dell Precision 490) but the outputs of each computer's video card (PC NVIDIA Quadro FX 5600) were frame-locked via NVIDIA Quadro G-Sync cards. The monitor screens were each 41.8 degrees wide and 32.0 degrees high, had 1024 × 768-pixel resolution (i.e. 23.4 pixels/degrees directly ahead of each eye), and the two were synchronously refreshed at a rate of 150 Hz. Each monitor was driven via an attenuator (Pelli, 1997) and a video signal splitter (Black Box Corp., AC085A-R2), allowing presentation of black/white images with 11-bit grayscale resolution (mean luminance of 20.8 cd/m^2). Visual stimuli were seen through an approximately 22 degrees by approximately 22 degrees (512 × 512 pixels) rectangular aperture centered directly ahead of the eyes.

Motion stimuli were vertical 1D binary pink noise patterns, constructed by randomly assigning a "black" or "white" value to each successive column of pixels. The one-dimensional Fast Fourier Transformation (FFT) along the axis of motion was then calculated, and each element of the FFT array was divided by the square root of the corresponding spatial frequency (Figure 1A). The inverse FFT restored the grey-scale stimulus (an example is shown in Figure 1B). Pink noise stimuli always had 32% root mean square (RMS) contrast. Noise patterns' motion was horizontal at approximately 13 degrees/s, approximately 25 degrees/s, approximately 51 degrees/s, or approximately 102 degrees/s (achieved by shifting an image by 2, 4, 8, or 16 pixels each video frame, respectively).

The motion stimulus was preceded by 600 to 1000 ms of maintained fixation (on a visible fixation cross), and we explored the effect of different stimuli—"fixation patterns"—presented during the fixation period on the OFRs to motion that followed. Six types of fixation patterns were implemented.

Blank screen: a grey screen with mean luminance (20.8 cd/m^2) and a fixation cross present. At fixation period end, a 32% RMS contrast 1D vertical pink noise sample (randomly selected from a lookup table) was

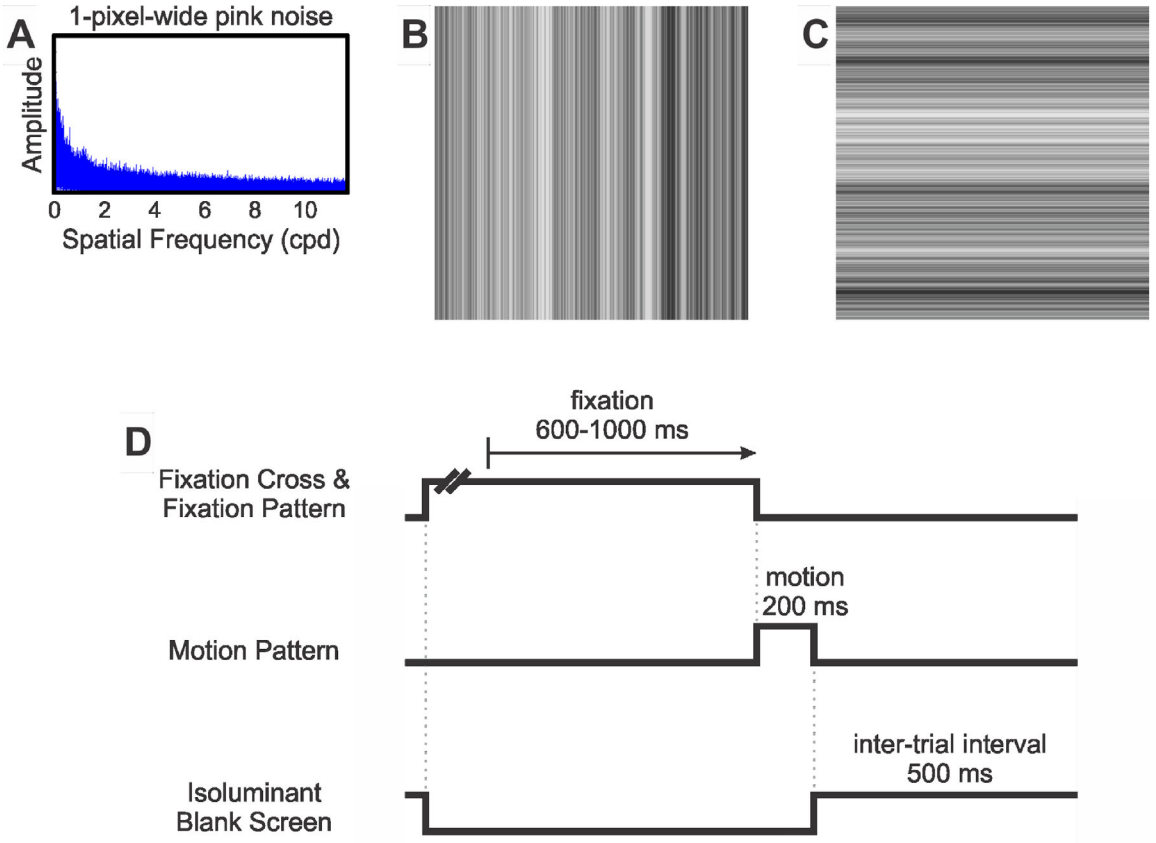

Figure 1. (**A**) Fourier composition of a 1D 1-pixel-wide pink noise stimulus. (**B**) An example of 32% RMS vertical 1D pink noise stimulus: a scaled version of a 22 degrees/22 degrees 1-pixel-wide pattern. Such stimuli were used as both fixation and (horizontal) motion patterns. (**C**) An example of 32% RMS horizontal 1D pink noise stimulus: a scaled version of a 22 degrees/22 degrees 1-pixel-wide pattern. Such stimuli were used as fixation patterns only. (**D**) Temporal sequence of events in an experimental trial.

presented and underwent the first step of horizontal motion one video frame later.

Random-Luminance blank screen: for the entire fixation period, the screen remained blank (apart from a fixation cross), although its luminance was changed every three video frames (i.e. at 50 Hz). Successive luminance values were randomly picked from the range of luminance levels of a randomly selected 32% RMS contrast 1D pink noise stimulus. At fixation period end, a 32% RMS contrast randomly selected 1D vertical pink noise sample was presented and underwent the first step of horizontal motion one video frame later.

Static 1D vertical pink noise: a 32% RMS contrast 1D vertical pink noise sample (an example is shown in Figure 1B) stayed on the screen for the entire fixation period. At its end, this sample was replaced by a new randomly selected 1D vertical pink noise sample, which underwent the first step of horizontal motion one video frame later.

Dynamic 1D vertical pink noise (vertical flicker): for the entire fixation period, a series of 32% RMS contrast 1D vertical pink noise samples (randomly selected from a lookup table) succeeded one another. Each sample stayed on the screen for three video frames (i.e. at 50 Hz). At fixation period end, the last sample in the series was replaced by a new randomly selected 1D vertical pink noise sample, which underwent the first step of horizontal motion one video frame later.

Static 1D horizontal pink noise: a 32% RMS contrast 1D horizontal pink noise sample (an example is shown in Figure 1C) stayed on the screen for the entire fixation period. At its end, this sample was replaced by a randomly selected 1D vertical pink noise sample, which underwent the first step of horizontal motion one video frame later.

Dynamic 1D horizontal pink noise (horizontal flicker): for the entire fixation period, a series of 32% RMS contrast 1D horizontal pink noise samples (randomly selected from a lookup table) succeeded one another. Each sample stayed on the screen for three video frames (i.e. at 50 Hz). At fixation period end, the last sample in the series was replaced by a randomly selected 1D vertical pink noise sample, which

underwent the first step of horizontal motion one video frame later.

A single block of trials had 48 randomly interleaved stimuli: six fixation patterns, four speeds of motion, and two motion directions (leftward or rightward).

Experiment 1A: In this short control experiment, only one eye (left or right) was shown the motion stimulus: 1D vertical pink noise stimuli moving horizontally at approximately 13 degrees/s or approximately 51 degrees/s; the screen seen by the other eye was mean luminance (20.8 cd/m^2) blank. Three pre-motion fixation conditions were used: blank screen for both eyes or dynamic 1D vertical pink noise for one eye while a blank screen for the other. Thus, a single block of trials had 12 randomly interleaved stimuli: three fixation conditions (no flicker, "same eye: flicker, and "other eye" flicker), two speeds of motion, and two directions of motion (leftward or rightward).

Procedures

Experimental paradigms were controlled by three PCs, which communicated via Ethernet (TCP/IP protocol). The first PC utilized a Real-time EXperimentation software (REX; Hays, Richmond, & Optican, 1982), which provided the overall control of the experimental protocol, acquisition, display, and storage of the eye-movement data. Two other PCs utilized the Psychophysics Toolbox extensions of Matlab (Brainard, 1997; Pelli, 1997) and generated the visual stimuli.

The temporal sequence of events in an experimental trial is shown in Figure 1D. At the start of each trial, a central fixation cross (width 10 degrees, height 2 degree, and thickness 0.2 degrees) appeared at the screen center, superimposed upon one of six implemented fixation patterns. After the subject's eye had been positioned within 2 degrees of the fixation target and no saccades had been detected (using an eye velocity threshold of 18 degrees/s) for a randomized period of 600 to 1000 ms, the fixation pattern and cross were replaced by the first frame of the (randomly selected) motion stimulus, whose first horizontal motion step commenced one video frame (6.7 ms) later. The motion lasted for 200 ms; the screen then turned to uniform gray (luminance = 20.8 cd/m^2) marking the end of the trial. A new fixation target appeared after a 500 ms inter-trial interval, signaling a new trial. The subjects were asked to refrain from blinking or shifting fixation except during the inter-trial intervals but were given no instructions relating to the motion stimuli. If no saccades were detected for the duration of the trial, then the data were stored; otherwise, the trial was aborted and repeated within the same block. Data collection usually occurred over several sessions until each condition had been repeated an adequate number of times to permit good resolution of the responses (through averaging).

Data analysis

The calibration procedure provided eye position data which were fitted with second-order polynomials and later used to linearize the horizontal eye position data recorded during the experiment. Eye-position signals were then smoothed with an acausal sixth order Butterworth filter (3 dB at 30 Hz) and mean temporal profiles were computed for each stimulus condition. Trials with micro-saccadic intrusions (that had failed to reach the eye-velocity cutoff of 18 degrees/s used during the experiment) were deleted. We utilized "position difference measures" to minimize the impact of directional asymmetries and boost the signal-to-noise ratio: the mean horizontal eye position with each leftward motion stimulus was subtracted from the mean horizontal eye position with the corresponding rightward motion stimulus. Mean eye velocity was estimated by subtracting position difference measures 10 ms apart (central difference method) and evaluated every millisecond. Response latency was estimated by determining the time after stimulus motion onset when the mean eye velocity first exceeded 0.1 degrees/s. The initial OFRs to a given stimulus were quantified by measuring the changes in the mean horizontal eye position signals—"OFR amplitude"—over the initial open-loop period (i.e. over the period up to twice the minimum response latency). This window always commenced at the same time after the stimulus onset ("stimulus-locked measures") and, for a given subject, was the same for different stimulus conditions of any given experiment reported in this paper. Bootstrapping procedures were used for statistical evaluation of the data and to construct 68% confidence intervals of the mean in the figures (these intervals were smaller than the symbol size in many cases and, therefore, not visible on most graphs).

Results

Panels A to C of Figure 2 show that the relationship between stimulus speed and OFR amplitude depends upon the pattern presented during fixation, prior to stimulus motion. These relationships were well described as a Gaussian function of log(speed; shown by continuous lines; r^2 range = 0.758–1.000; median r^2 = 0.983, 0.950, and 0.926 for subjects BMS, EJF, and TH, respectively). The amplitude of OFRs with static noise fixation patterns (shown by filled symbols) were affected the least, showing only an 18% attenuation relative to the blank screen fixation condition (purple filled squares). Moreover, in subject EJF, the differences in the OFR amplitude between the blank screen and

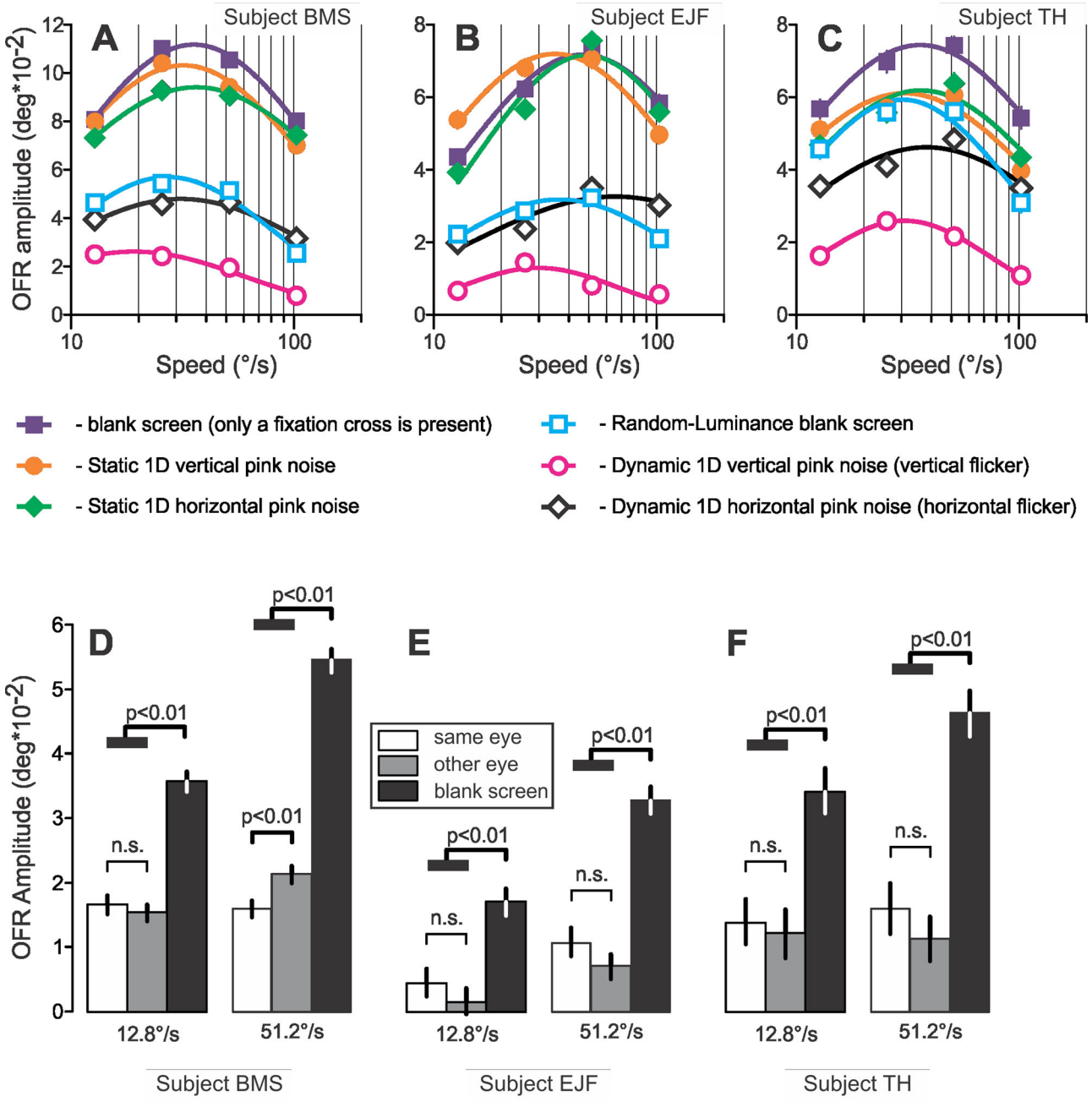

Figure 2. Experiment 1. (**A–C**) OFR amplitude dependencies upon the speed of 1D vertical pink noise motion following six different fixation conditions, shown by different symbols: see legend. Symbols: data; solid smooth lines: Gaussian fits. (**D–F**) Experiment 1A. OFR amplitudes to monocular motion stimuli. White vertical bars: Dynamic 1D vertical pink noise fixation pattern for the eye that subsequently was shown motion stimulus, while blank screen fixation pattern for the other eye. Grey vertical bars: Blank screen fixation pattern for the eye that subsequently was shown motion stimulus, whereas dynamic 1D vertical pink noise fixation pattern for the other eye. Black vertical bars: Blank screen fixation patterns in both eyes. (**A, D**) Subject BMS; (**B, E**) subject EJF; and (**C, F**) subject TH. Thin vertical lines: 68% confidence intervals of the mean (bootstrapping). In many cases in **A–C**, these intervals were smaller than a symbol size and, thus, not visible on the graphs.

either of static noise fixation conditions were not statistically significant. Dynamic fixation patterns (shown by open symbols) resulted in a more substantial drop in the OFR amplitude. Horizontally oriented flickering fixation patterns (dynamic 1D horizontal pink noise; black open diamonds); i.e. the ones whose orientation was orthogonal to that of motion patterns led to a 38% to 57% drop in the OFR amplitude. Vertically oriented flickering fixation patterns (dynamic 1D vertical pink noise; pink open circles; i.e. the ones

whose orientation matched that of motion patterns) were the most detrimental: 65% to 82% OFR amplitude drop. OFR amplitudes in random-luminance blank screen condition (blue open squares) were similar to those observed with the dynamic 1D horizontal pink noise in subjects BMS and EJF (49% and 56% drop, respectively), where as in subject TH they were on par (20% drop) with the OFR amplitudes recorded with static noise fixation patterns (18% and 17%). For the most part, the best-fit values of the other two Gaussian parameters—offset and standard deviation—did not show statistically significant changes with the fixation pattern, although the dynamic 1D vertical pink noise and random-luminance blank screen in subject BMS, as well as the static 1D vertical pink noise in subject EJF, resulted in the Gaussian peaks being shifted toward lower speeds than in the blank screen fixation condition.

Some of these suppressive effects might be explained by adaptation phenomena as early as the retina. In order to assess this, we examined the strongest suppression (dynamic vertical noise) under dichoptic conditions: the fixation pattern and the motion stimulus were monocular, shown either to the same eye or to different eyes (Experiment 1A; Figures 2D–F). Compared to a blank screen fixation pattern, OFRs were strongly attenuated ($p < 0.01$) in both cases, and the same eye condition (white bars) produced significantly smaller responses than the opposite eye condition in only one instance (subject BMS, 51.2 degrees/s). Thus, this suppression is largely dependent on a binocular stage, presumably reflecting a cortical substrate.

Discussion

We show that presenting a wide range of temporally modulating patterns during fixation substantially attenuates OFRs to subsequently presented motion stimuli. Conversely, static patterns produce little attenuation. Both types of patterns had the same contrast, so if this reflects a form of contrast adaptation it would have to be adaptation to spatiotemporal contrast (Pantle, 1971; Smith, 1970). In all subjects, a flicker orthogonal to the axis of stimulus motion produced less OFR attenuation that the one matching it (see Figures 2A–C: black open diamonds versus pink open circles), which suggested that the attenuation mediating circuits were at least partially orientation selective. Nonetheless, it is striking that orthogonal patterns produce at least half as much attenuation as parallel patterns, so the orientation tuning is very broad. This might suggest an interaction at an early stage (before striate cortex) but the fact that the attenuation is unaffected by dichoptic presentation (see Figures 2D–F) argues for a cortical substrate. The broad orientation selectivity presumably reflects pooling across orientation selective channels.

In the blank screen condition, preferred speeds were 30 to 50 degrees/s (purple filled squares and lines in Figures 2A–C). This is similar to what was reported in earlier studies performed on human subjects using random dot patterns (Gellman et al., 1990) and 1D white noise (Sheliga, Quaia, FitzGibbon, & Cumming, 2016). However, to our knowledge, this is the first description of speed tuning with 1D pink noise patterns.

Experiment 2

One simple explanation for the OFR attenuation found in Experiment 1 is that the fixation patterns produce adaptation in spatiotemporal channels, so the adapted channels then produce smaller responses when the motion stimulus starts. Alternatively, we recently showed that flickering patterns suppress the OFR at short latency (Sheliga et al., 2016) – a similar suppressive mechanism, if it persists over time, might explain the results above. The suppression was selective for the SF of the flickering pattern, largely independent of the frequency of the motion stimulus (unlike adaptation; figure 4 in Sheliga et al., 2016). Thus, how the attenuation generated by fixation patterns depends upon SF can help differentiate these two explanations. Experiment 2 examines this question.

Materials and methods

Only methods and procedures that were different from those used in Experiment 1 will be described.

Visual stimuli

Both motion stimuli and fixation patterns were constructed from 1D pink noise (as described in Experiment 1) that was then bandpass filtered. We refer to these as 1D noise below for simplicity. The band-pass filter was a Gaussian function of log frequency. The central SF of the filter varied (see below), whereas the full width at half maximum (FWHM) was always set to two octaves (De Valois, Albrecht, & Thorell, 1982). With the bandwidth fixed on a log-scale, filtered pink noise patterns with different central SFs had the same RMS contrast. The motion stimuli were 1D vertical noise patterns, moving horizontally. The speed of each stimulus was chosen such that its central SF moved at 18.75 Hz (45 degrees phase shift each video frame), which is a near-optimal temporal frequency for evoking the OFRs (Gellman et al., 1990; Sheliga et al., 2016). Motion was preceded by 600 to 1000 ms of fixation. Two different temporal structures for the

fixation pattern were explored. In Experiment 2A, the fixation pattern was flickering (temporally broadband). In Experiment 2B, the fixation pattern consisted of transparent motion in opposite directions, so the temporal frequency (TF) content matched that of the subsequent motion stimulus.

Experiment 2A – dynamic fixation pattern: During the fixation period, a series of 1D horizontal (or vertical) samples (randomly selected from a lookup table) succeeded one another. Each sample stayed on the screen for three video frames (i.e. at 50 Hz) and had RMS contrast approximately 13%. At the fixation period end, the last sample in the series was replaced by a randomly selected filtered 1D vertical noise sample, which underwent the first step of horizontal motion one video frame later. In different trials, the central SF of the filter varied from 0.125 to 1 cpd (motion stimuli) and from 0.0625 to 2 cpd (fixation patterns), in octave increments[1]. The fixation pattern stayed on the screen throughout the fixation period. In one fixation condition, the pattern was a single static 1D (horizontal or vertical) full pink noise stimulus with 32% RMS contrast. Horizontal and vertical fixation patterns were run in different experimental sessions. The static vertical 1D full pink noise pattern followed by motion of a 0.25 cpd central SF stimulus was included in all sessions, and the amplitude of this response was used to normalize responses across sessions when quantitative comparisons were made between them. A single block of trials had 56 (or 58, if the common condition had to be added) randomly interleaved stimuli: seven fixation conditions, four central SFs of motion stimuli, and two motion directions (leftward or rightward).

Experiment 2B fixation pattern with transparent motion: The fixation pattern was the sum of two 1D noise patterns (each 10% RMS contrast) moving in opposite directions (either vertically or horizontally). The speed was chosen such that the central SF had a TF of 18.75 Hz. At the end of the fixation period, a randomly selected filtered 1D vertical noise sample was presented and underwent the first step of horizontal motion one video frame later. In different trials, the central SF of the filter varied from 0.18 to 1.46 cpd (motion stimuli) and from 0.09 to 2.93 cpd (fixation patterns), in octave increments[2]. In addition to four SFs of the transparently moving fixation pattern, we also measured responses following a static fixation pattern, to facilitate comparisons with other sessions. To avoid any frequency-specific effects, the SF of this static fixation pattern was chosen randomly (on each trial) for the set of SFs used across all trials. In sessions recording responses with horizontal fixation patterns, we included one stimulus with a static vertical fixation pattern followed by a moving stimulus at 0.37 cpd. Because this stimulus was used in both types of sessions (vertical or horizontal fixation patterns), it served as a reference stimulus to allow normalization when comparing data collected from different sessions. A single block of trials had 56 (or 58, if the reference condition had to be added) randomly interleaved stimuli: seven fixation conditions, four central SFs of motion stimuli, and two motion directions (leftward or rightward).

Results and discussion

Figure 3 shows the results of Experiments 2A and 2B for three subjects. For each subject, four sets of data are shown: the upper row shows Experiment 2A (flicker), the lower row shows Experiment 2B (transparent motion); the left column—"Orthogonal Orientation"—shows the OFRs recorded when the fixation pattern was horizontal and the motion pattern was vertically oriented; the right column—"Same Orientation"—shows the OFRs recorded when both epochs contained vertically oriented stimuli. Each panel shows the OFR amplitude as a function of the central SF of motion noise patterns (on log abscissa). Different symbols show the data for dynamic fixation patterns of different central SF (see Figure 3 legend). The OFRs recorded with static fixation patterns are not shown. They were larger than those to dynamic patterns[3], and their SF tuning dependencies were very well fit by semi-log Gaussian functions (median $r^2 = 0.992$, range = 0.902–1.000), as was always the case for pure sine wave gratings in our earlier studies (Sheliga et al., 2005; Sheliga, Quaia, Cumming, & Fitzgibbon, 2012).

Two features of the data are evident in Figure 3. First, OFR amplitudes are smaller when the fixation pattern has the same orientation as the motion one (i.e. in the same orientation case; compare the data in right and left columns of each subject's data). Second, the most effective moving SF changes as a function of the fixation SF, most clearly seen in the same orientation cases. The first step in quantitative data analysis was an evaluation if the observed OFRs were a separable function of the two SFs (fixation and motion). For this, we fitted the dataset for each orientation case (orthogonal orientation and same orientation) in each Experiments 2A and 2B with an arbitrary function of fixation SF (i.e. allowing n free parameters for n fixation SFs), and an arbitrary function of motion SF (i.e. allowing m free parameters for m motion SFs), to find the best fitting separable description of the data. That is, any n data points for fixation SF alone would be perfectly fit with our n parameters – the n parameters are simply the n response amplitudes. In this approach, the fitted response to a given combination of the fixation and motion SFs is calculated as a product of the two corresponding free parameters. By allowing both of these functions to take any form, we ensure that any failure in fitting is the result only of inseparability in the data. The r^2s of such fits were rather high: median $r^2 = 0.916$; range 0= .818–0.970. The r^2 values

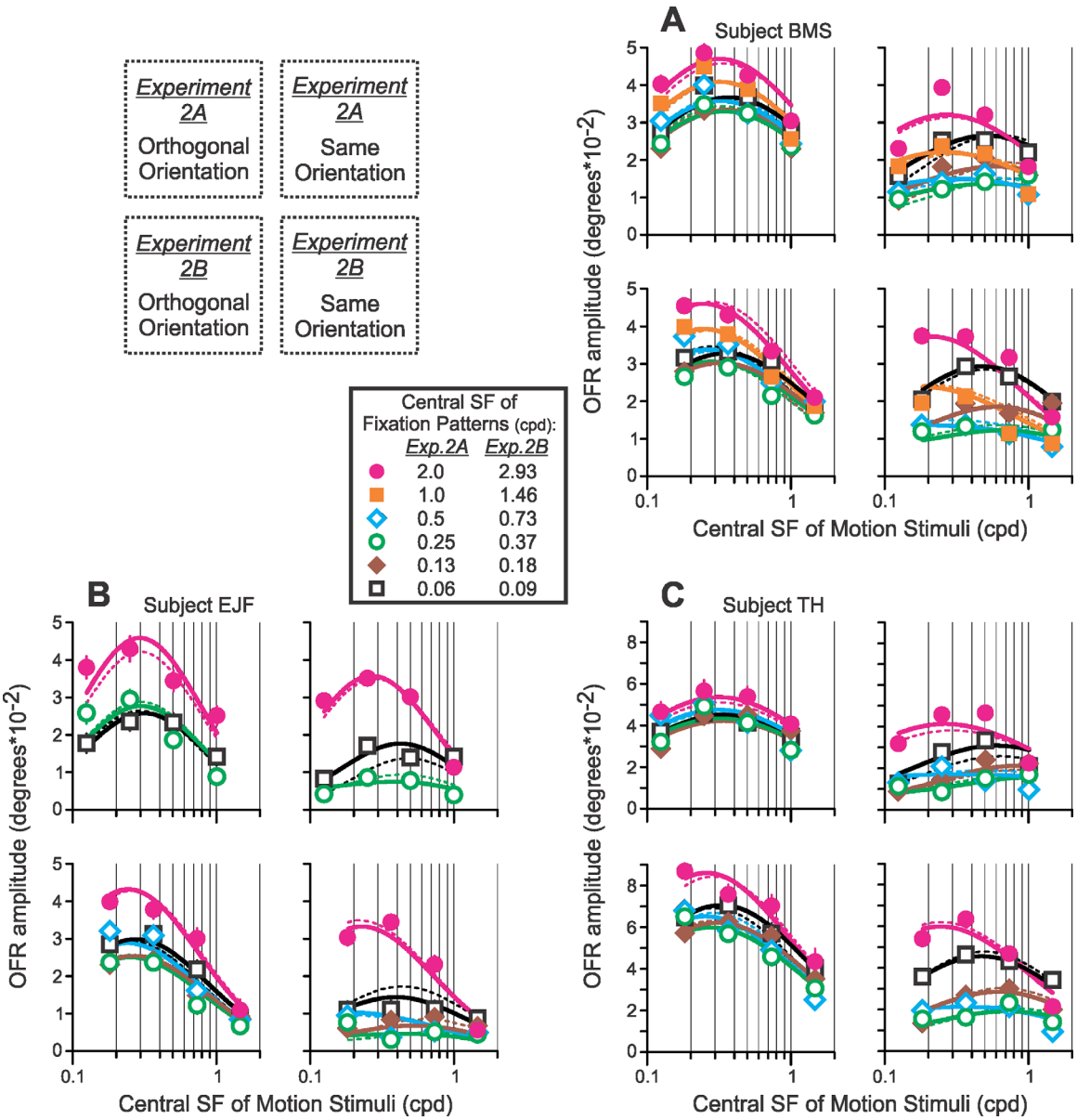

Figure 3. Experiment 2. Three quartets of panels (**A**, **B**, **C**) display the data of three subjects. Each panel shows the OFR amplitude dependence upon the central SF of moving 1D vertical band-pass pink noise pattern (on log abscissa). A diagram in the upper left corner illustrates data arrangement. Upper row: Experiment 2A; lower row: Experiment 2B. Left column: Orthogonal Orientation (the orientations of the fixation and moving patterns were orthogonal; i.e. horizontal versus vertical, respectively); right column: Same Orientation (the orientations of the fixation and moving patterns were the same; i.e. vertical). Fixation patterns of different central SF are shown by different symbols: see figure legend. Equation 1b fits obtained using 20 free parameters are shown by solid lines, while those using seven free parameters are shown by thinner dashed lines. See text for further explanations. Thin colored vertical lines: 68% confidence intervals of the mean (bootstrapping).

were somewhat higher for the orthogonal orientation cases (median $r^2 = 0.943$) than for the same orientation ones (median $r^2 = 0.872$): this modest difference in r^2 values was statistically significant ($p < 0.05$) in three of six cases, and unlikely to be of much importance. These high r^2 values clearly show that a great deal of variability in the data of each relative orientation case of Experiments 2A and 2B can be explained using separable functions of the fixation and motion SFs. As an illustration, Figures 4A, B show the best-fit values of n and m free parameters, respectively, for subject BMS. In each of four experimental configurations (2 orientation cases in 2 experiments) this subject was tested using six fixation SFs ($n = 6$) and four motion SFs ($m = 4$). In Figure 4A, the values of six "fixation" best-fit free parameters are plotted as a function of

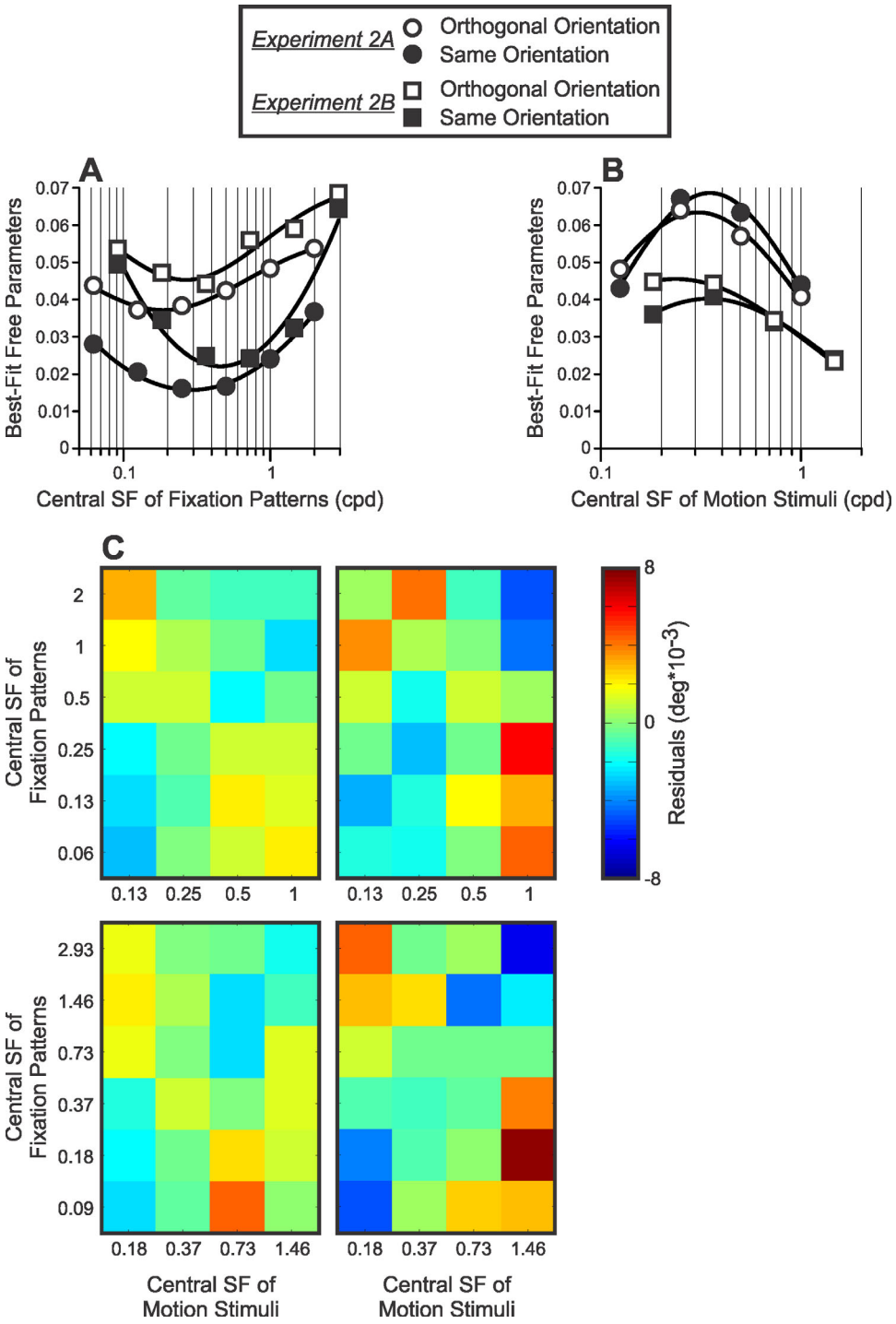

Figure 4. Experiment 2. An example (subject BMS) of data analyses which used separable (**A**, **B**) and inseparable functions (**C**) of the fixation and motion SFs. See text for details. (**A**) "Fixation" best-fit free parameters plotted as a function of the fixation pattern SF. (**B**) "Motion" best-fit free parameters plotted as a function of the motion stimulus SF. (**C**) A two-dimensional checkerboard—fixation versus motion SFs—of residuals which result when the best-fit values of the fits of separable functions, shown in **A** and **B**, are subtracted from the OFRs actually recorded during the experiments.

the fixation SF. All four dependencies (2 orientation cases in 2 experiments) are very similar: a trough at intermediate fixation SFs, with values rising toward lower and higher SFs. In fact, all of them were very well fit by inverted Gaussian functions (r^2 range = 0.945–0.993; solid lines). In Figure 4B, the values of four "motion" best-fit free parameters are plotted as a function of motion SF. Again, all four dependencies are very similar: a peak value at intermediate motion SFs, with values falling toward lower and higher SFs. They were well fit by Gaussian functions (r^2 range = 0.982–0.998; solid lines) and are very similar to the dependencies we usually see for the OFR SF tuning (Sheliga et al., 2005; Sheliga et al., 2012). Thus, in the full model, which will be presented below, we will substitute "arbitrary functions" of fixation and motion SFs with Gaussians (*G1* and G_{OFR}, respectively, see below). However, Figure 4C suggests that an inseparable function of the fixation and motion SFs also plays a role. As an illustration, Figure 4C plots a two-dimensional checkerboard—fixation versus motion SFs—of residuals, which result when the OFR's amplitudes obtained using best-fit values of the separable functions of the fixation and motion SFs outlined above are subtracted from the OFRs actually recorded during the experiments for subject BMS. In all four panels (arranged as in Figure 3A) one can observe a similar structure: the fits overestimate the OFR amplitudes for the fixation/motion SF combinations along the unity line (bluish squares; see the color bar on the right) and underestimate them on the sides (yellowish and reddish squares). These effects appear to be weaker in the orthogonal orientation cases (left column) than in the same orientation ones (right column), an observation which complements higher r^2 values obtained for the orthogonal versus same orientation conditions when we attempted the description of the data by separable arbitrary functions of the fixation and motion SFs as described above.

These analyses led us to formulate a model, which posits that the OFRs in Experiments 2A and 2B can be accounted for using three functions, namely, G_{OFR} (a function of motion SF), *G1* (a function of fixation SF), and *G2* (an inseparable function of fixation/motion SFs):

$$\mathrm{OFR} = G_{OFR}{}^{*}\,(1 - G1 - G2) \quad (1a)$$

or

$$\mathrm{OFR} = G_{OFR}{}^{*}\,(1 - S^{*}G1^{*}G2) \quad (1b)$$

In Equation 1b, G1 and G2 have unity amplitude, and the term S scales the amplitude of the attenuation.

$G_{OFR}(SF_M)$ is a Gaussian function of (log)SF—OFR SF tuning function—which describes the OFR amplitudes as a function of motion SF in blank screen condition (i.e. when there was no fixation pattern during the fixation period):

$$G_{OFR}(SF_M) = \lambda_{OFR} * e^{-\frac{\left[\log_2(SF_M)-\mu_{OFR}\right]^2}{2*\sigma_{OFR}{}^2}} \quad (2)$$

Equation 2 has three free parameters: λ_{OFR}, μ_{OFR}, and σ_{OFR}. We, however, constrained μ_{OFR} and σ_{OFR} to be equal to the best-fit values of the OFR SF tuning function for the static condition in the orthogonal orientation case, because we did not have the blank screen condition in Experiments 2A and 2B. We felt that doing so was justified because in Experiment 1 the speed tuning for these two conditions was very similar (see Figure 2). The value of λ_{OFR} was also constrained, but its estimation was slightly indirect. We exploited the fact that in Experiment 1 OFR amplitudes following the orthogonal orientation static patterns were very similar to those following the blank screen condition (see Figure 2). We took the best-fit λ_{OFR} value of the OFR SF tuning function for the static condition in the orthogonal orientation case and then multiplied it by ratio of the amplitudes found in Experiment 1. So, the parameters in Equation 2 were fixed using data that was not used to constrain the other parameters.

$G1(SF_F)$ is a Gaussian function of (log)SF, which describes the scaling of OFRs as a function of fixation pattern SF, regardless of the orientation or SF of the motion pattern:

$$G1\,(SF_F) = \lambda_{G1} * e^{-\frac{\left[\log_2(SF_F)-\mu_{G1}\right]^2}{2*\sigma_{G1}{}^2}}, \quad (3)$$

with λ_{G1}, μ_{G1}, and σ_{G1} as three free parameters.

$G2(SF_F;SF_M)$ is a Gaussian function of the log ratio of fixation/motion SFs:

$$G2\,(SF_F;\,SF_M) = \lambda_{G2} * e^{-\frac{\left[\log_2\left(K_{G2}*\frac{SF_M}{SF_F}\right)\right]^2}{2*\sigma_{G2}{}^2}}, \quad (4)$$

with λ_{G2}, σ_{G2}, and K_{G2} as free parameters. K_{G2} free parameter was required to accommodate the possibility of Equation 4 reaching maximum when $SF_M \neq SF_F$.

For each subject, we fitted all the data in Experiments 2A and 2B (each quartet of plots in Figure 3) by Equations 1a and 1b. Equation 1a had 24 free parameters: four experiments times two Gaussian fits (G1 and G2) times three free parameters per Gaussian fit. Equation 1b had 20 free parameters: four experiments times two Gaussian fits (G1 and G2) times two free parameters per Gaussian fit ($\lambda_{G1} = \lambda_{G2} = 1$), plus a free scaling parameter *S* for each experiment (totaling 4). Thus, 24 free parameters (Equation 1a)

	S				σ (log2 units)		μ_{G1} (cpd)		K_{G2} (Same orientation case; log2 units)	r^2
	Orthogonal		Same							
Subject	Exp. 2A	Exp. 2B	Exp. 2A	Exp. 2B	G1	G2	Orthogonal	Same		
BMS	0.48	0.62	0.87		3.7	5.3	0.16	SF tuning	1.4	0.921
EJF	0.48	0.59	0.96		3.1	5.0	0.09		1.0	0.921
TH	0.19	0.41	0.90		2.8	4.7	0.12		1.7	0.939

Table 1. Experiment 2: The best-fit values of free parameters for Equations 1-4.

and 20 free parameters (Equation 1b) allowed separate sets of free parameters for each experiment. For a moment, we proceed with both equations because our simulations showed that they would have produced similar results. The fits were quite good: Equation 1a $r^2 = 0.942$, 0.944, and 0.954; Equation 1b $r^2 = 0.939$, 0.940, and 0.955 for subjects BMS, EJF, and TH, respectively. In subjects BMS and EJF, the r^2 values of fits produced by Equation 1b (20 free parameters) were slightly lower than those produced by Equation 1a (24 free parameters), but this deterioration of fits was not statistically significant—general linear F-test: F(4,72) = 0.81 and F(4,40) = 0.72 for subjects BMS and EJF, respectively. The fits for Equation 1b are shown by solid lines in Figure 3. For Equation 1b, an inspection of the best-fit values revealed several similarities between the corresponding free parameters of Experiments 2A and 2B, as well as between free parameters comprising each experiment's set: (a) *S* in the same orientation case of Experiments 2A and 2B; (b) μ_{G1} and μ_{OFR} in Experiment 2B; (c) μ_{G1} in the same orientation and orthogonal orientation cases of Experiment 2A; (d) K_{G2} in Experiments 2A and 2B; (e) σ_{G1} and σ_{G2} in the same orientation and orthogonal orientation cases of each experiment and between Experiments 2A and 2B. We constrained pairs of parameters listed in (a) to (d) and four parameters listed in (e) to be the same. We also assumed that the *G2* function does not operate in the orthogonal orientation case. This led to a reduction in the number of free parameters from 20 to seven. The fits were little changed ($r^2 = 0.921$, 0.921, and 0.939 for subjects BMS, EJF, and TH, respectively): see dashed thinner lines in Figure 3, and the deterioration of fits was not statistically significant—general linear F-test: F(13,76) = 1.72, F(13,44) = 1.07, F(13,60) = 1.63 for subjects BMS, EJF, and TH, respectively. The best-fit values of free parameters are listed in Table 1. For Equation 1a, an inspection of 24 best-fit values revealed many similarities as well. However, the deterioration of fits due to a reduction in the number of free parameters was more severe, and their number could not be reduced to less than nine. We, therefore, dropped Equation 1a as a potential framework for the explanation of the results for Experiments 2A and 2B.

In both experiments, the strength of *G1* suppression depended exclusively on the central SF of the fixation pattern, and the dependence was a Gaussian function of log(SF). In all three subjects, in the orthogonal orientation case, this suppression was stronger in Experiment 2B than in Experiment 2A. In Experiment 2B (transparent motion) it peaked at the same SF as the OFR SF tuning curve (i.e. $\mu_{G1} = \mu_{OFR}$; 0.33, 0.29, and 0.32 cpd for subjects BMS, EJF, and TH, respectively). In Experiment 2A (i.e. with flicker fixation patterns), the peak occurred at lower SFs (0.16, 0.09, and 0.12 cpd for subjects BMS, EJF, and TH, respectively). That a simple change in temporal structure produces this change in SF tuning suggests that the underlying mechanism is quite different from that which drives the OFR—which has separable tuning for SF and TF (Sheliga et al., 2016)—suggesting that the similarity between the OFR and the suppression in Experiment 2B is probably coincidental.

The *G2* suppression behaves as an orientation selective component of suppression, because it had to be called for only in experimental conditions in which the orientations of fixation and moving patterns were the same. Its strength was determined by the ratio of the fixation and motion patterns' central SFs, and the dependence had a Gaussian envelope (on log scale; see Equation 4). Surprisingly, the suppression was maximal when the SF of the moving pattern was much lower (2.6, 2.0, and 3.3 times) than that of the fixation one, and it is not trivial to imagine a mechanism which would account for such a mismatch. However, this finding mimics similar observations made in earlier MAE experiments (Ledgeway & Hutchinson, 2009; von Grunau & Dube, 1992); although in these latter studies the mismatch only developed for higher SF adapting stimuli. Hutchinson and Ledgeway (2007) observed similar phenomenon while measuring the SF tuning of motion detection mechanisms using the technique of visual masking. In those experiments, the mismatch was found with large stimuli (20 × 20 degrees, close to stimulus size in our study as well), but not with small ones (2.5 × 2.5 degrees). In 2009, they reasoned that "our adaptation results, like those revealed by masking, appear to be mediated by image size" (Ledgeway & Hutchinson, 2009). This dependence on stimulus size

might suggest that response normalization mechanisms are subject to the adaptive changes as well (Solomon & Kohn, 2014). Similarly, single unit recordings in macaque area MT in speed adaptation studies revealed that the suppression of neural activation to motion of random dot patterns was usually maximal when the adaptation and test speeds were different (Krekelberg, van Wezel, & Albright, 2006; Priebe & Lisberger, 2002; J. Yang & Lisberger, 2009). Priebe and Lisberger (2002) concluded "that the distribution of the ratio of the preferred adaptation and response speeds was broad and skewed slightly toward adaptation preferred speeds that were greater than response preferred speeds." Yang and Lisberger (2009), on the other hand, showed that the suppression was maximal when the adaption speed was approximately twice that of the test one (i.e. the effects were the most severe when the adapting stimulus activated lower SF circuits than those engaged during the test phase). Forcing the suppression to be maximal when central SFs of fixation and motion patterns were the same (removing the parameter K_{G2}) significantly worsened the fits—$F(1,89) = 53.8$, $F(1,57) = 9.55$, $F(1,73) = 41.1$—increasing the error by 60%, 17%, and 56% for subjects BMS, EJF, and TH, respectively.

To summarize, Equation 1b provided a single descriptive framework for the suppressive effects of two very different types of fixation patterns: flicker (Experiment 2A) and a pair of spatially superimposed patterns moving in opposite directions (Experiment 2B). The suppression was SF selective and had two components, one of which appears to be also orientation selective.

Experiment 3

Because Experiment 2 reveals a component of suppression that depends on both relative orientation and relative SF, it is natural to ask if the suppression might also be specific for the direction of motion. This is more difficult to explore, because a moving pattern presented during the fixation period would engage the OFR itself. However, we can exploit the dependence on relative SF to reveal a selectivity for direction of motion in the following way. The fixation pattern consists of transparent motion, with stimuli of different SF moving in the two directions. This is then followed by a moving pattern composed of one of the two SFs present during fixation, moving either in the same, or the opposite, direction.

Materials and methods

Only methods and procedures that were different from those used in Experiments 1 and 2 will be described.

Visual stimuli

One-dimensional noise patterns were constructed as described under Methods in Experiment 2B. During the fixation period, a pair of spatially overlapping patterns (randomly selected from a lookup table) moved horizontally in opposite directions (at 18.75 Hz for the central SF; 45 degrees phase shift each video frame). The central SF of the first pattern (OPT; i.e. "optimal") was set at 0.41, 0.38, and 0.43 cpd for subjects BMS, EJF, and TH, respectively. Stimuli of these SFs would cause OFRs of near-maximal amplitude if presented in isolation. The central SF of the second pattern was set four times higher (HIGH) or lower (LOW). The RMS contrast was 5% for OPT and 2.5% for HIGH/LOW. Pilot experiments showed that making the contrasts of HIGH/LOW smaller than that of OPT resulted in more robust effects. At fixation period end, one of the patterns was removed (as was the fixation cross), whereas the second one was substituted by a new randomly selected noise sample, which had the same central SF, although higher contrast (OPT ~20%; HIGH/LOW ~10%). This new sample—motion stimulus—underwent the first step of horizontal motion one video frame later in the direction, which was either the same (SAME) or opposite (FLIP) to the one that the pattern of this central SF had during the fixation period. We used higher contrasts for motion stimuli to obtain OFRs of larger amplitude. Fixation patterns also included static conditions (STATIC), in which spatially overlapping OPT and HIGH/LOW patterns stayed on the screen (w/o motion) for the duration of the fixation period.

Data analysis

As in Experiments 1 and 2, the OFRs were accessed using "position difference measures": the mean horizontal eye position with each leftward motion stimulus was subtracted from the mean horizontal eye position with the corresponding rightward motion stimulus. However, for SAME and FLIP, the "corresponding" conditions were those in which the motion stimulus and the corresponding component of the fixation pattern moved in the same and opposite directions, respectively.

Results and discussion

Figure 5 shows the results of Experiment 3 for three subjects (panels A, B, and C). In each panel, the upper row shows results when the fixation pattern consisted of OPT and LOW frequencies, whereas the lower row shows OPT and HIGH. OPT was the motion stimulus for the data shown in the left column, LOW (upper row) or HIGH (lower row) - for the data in the right column. Each trace shows mean OFR velocity profile, starting

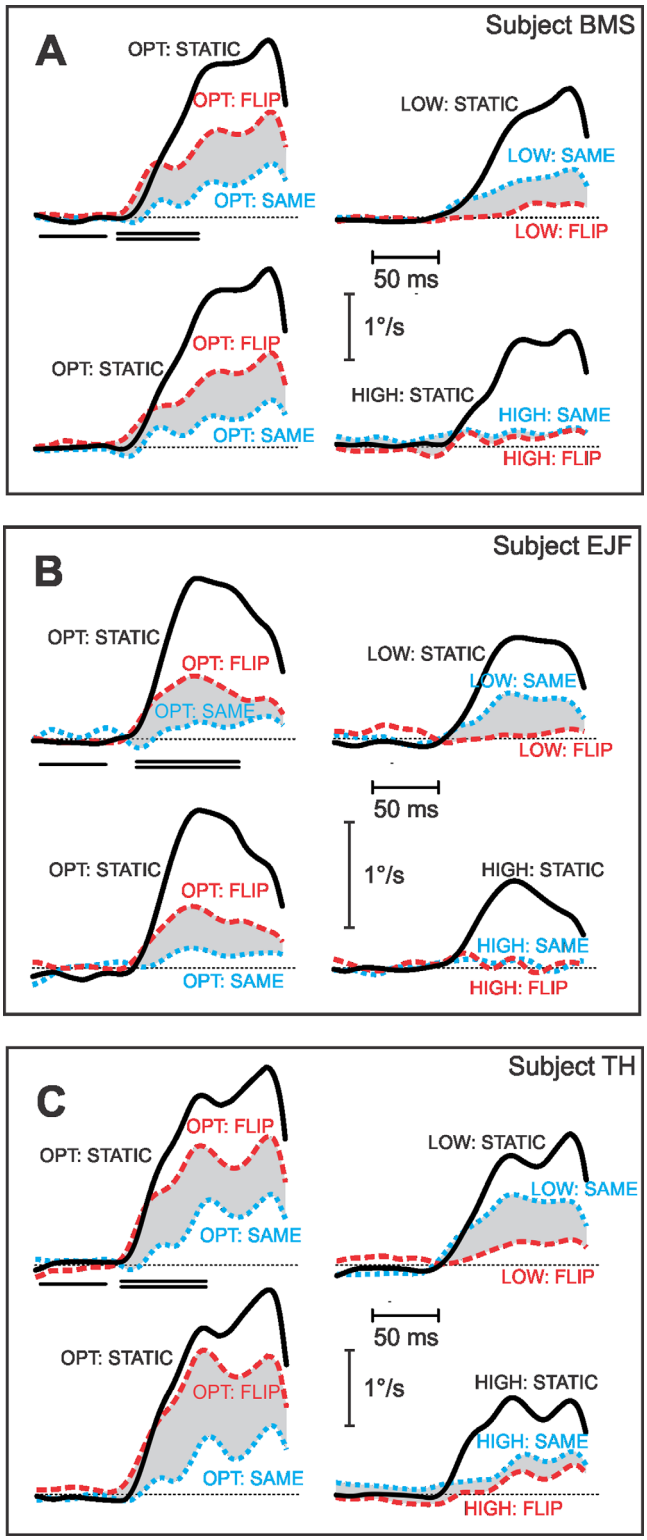

Figure 5. Experiment 3. Mean OFR eye velocity profiles over time to a pair of spatially overlapping 1D vertical band-pass filtered pink noise patterns, which moved horizontally in opposite directions. Quartets of panels—**A**, **B**, and **C**—display the data of three subjects. In each quartet, OPT and LOW comprised fixation patterns for the data shown in the upper row, OPT and HIGH – in the lower row. OPT was the motion stimulus for the data shown in the left column, LOW (upper row) or HIGH (lower row) – in the right column. Static fixation patterns = black solid traces; FLIP conditions = red dashed traces; SAME conditions = blue dotted traces. Each trace is the mean response to 98 to 130 stimulus repetitions. The abscissa shows the time from stimulus onset; horizontal thin dotted black line represents zero velocity. Double horizontal lines beneath the traces - response measurement window to motion stimuli; single horizontal lines beneath the traces - response measurement window of the prestimulus drift.

from the moment in time when the motion stimulus was presented. The dynamic fixation patterns (dotted-blue and dashed-red traces) resulted in much lower OFR velocities to motion stimuli than the static ones (black solid traces). As described in Methods, we quantified these observations by calculated the OFR amplitude to motion during the open-loop period, whose start and duration for each subject are indicated below the upper left panel of A, B, and C in Figure 5 by double horizontal lines. When compared to static fixation patterns, the dynamic fixation patterns resulted in 7% to 100% OFR amplitude drop that was statistically significant in 22 out of 24 cases. This result echoes observations made in Experiments 1 and 2. However, there was also a clear effect of the relative direction between fixation and motion stimuli. With OPT motion stimuli, responses were weaker when motion stimulus direction was the same as that of the fixation pattern OPT component (SAME; dotted-blue traces) than when motion stimulus direction was opposite to that of the fixation pattern OPT component (FLIP; dashed-red traces): a drop of 73% to 81%; statistically significant in all six cases ($p < 0.001$). With LOW motion stimuli the reverse was true: responses were weaker when motion stimulus direction was opposite to that of the fixation pattern LOW component (FLIP) than when motion stimulus direction was the same as that of the fixation pattern LOW component (SAME): a drop of 75% to 100%; statistically significant in all three cases ($p < 0.001$). Following the dynamic fixation patterns, the OFRs to HIGH motion stimuli were always extremely weak in all three subjects, although in two of them (subjects BMS and TH) the pattern of results replicated that found with LOW motion stimuli (i.e. the OFRs were statistically significantly weaker in the FLIP than in the SAME condition, $p < 0.001$).

Thus, although the results with the OPT moving stimulus could be explained by adaptation in spatiotemporal channels, the results with LOW moving stimuli have the opposite pattern to that expected. One way of describing both patterns is that the response to moving stimuli in the same direction as the OPT fixation component are suppressed, over a broad range of SFs. This may reflect an MAE with an unusually broadband influence. Or it could be a result of processes required to maintain fixation while viewing our stimuli.

During this time, the OPT component produces the strongest drive due to both its higher contrast (Sheliga, Kodaka, FitzGibbon, & Miles, 2006) and its SF (Sheliga, Quaia, FitzGibbon, & Cumming, 2020). This would normally result in an OFR in the direction of the OPT component. It may be that maintaining fixation here requires a suppression of motion signals in the OPT direction. If this direction-specific suppression were to affect subsequent motion stimuli over a broad range SFs then, when a requirement to fixate is lifted, the OFRs to OPT motion stimulus should be stronger in the FLIP than in the SAME condition. Conversely, the OFRs to LOW/HIGH motion stimuli should be stronger in the SAME than in the FLIP condition. This is exactly what Figure 5 shows.

A careful inspection of Figure 5 suggests that there were tiny drifts of the eyes during the fixation period. That is the velocity during the first 60 to 70 ms (prior to the OFR latency) was not quite identical during the STATIC, SAME, and FLIP conditions. However, these differences are much smaller than those that emerge after the OFR latency (and often have the opposite sign). It therefore seems unlikely that small drifts produced by the fixation stimulus are responsible for the differences we see in these OFRs.

Experiment 4: Time course of OFR suppression

Materials and methods

Only methods and procedures that were different from those used in Experiment 1 will be described.

Visual stimuli

The 1D vertical pink noise patterns were constructed as described in Methods of Experiment 1. The duration of the fixation period was fixed at 640 ms. This time interval was subdivided into two stages, during which static 1D vertical pink noise and dynamic 1D vertical pink noise (vertical flicker) fixation patterns were shown (see Methods of Experiment 1). The static pattern (stage 1) was followed by the dynamic one (stage 2), or vice versa. In different conditions, the duration of stage 2 was set to 20, 40, 80, 160, or 320 ms (Figure 6A). Two more fixation conditions were also included: static only and dynamic only, during which static or dynamic fixation patterns, respectively, were shown for the entire duration of the fixation period (i.e. stage 2 duration of 0 ms). At fixation period end, a new randomly selected 1D vertical pink noise sample was put on the screen and underwent the first step of horizontal motion one video frame later. Motion speed was set to approximately 13 degrees/s or approximately 51 degrees/s (achieved by shifting the image by 2 or 8 pixels each video frame, respectively).

A single block of trials had 48 randomly interleaved stimuli: six durations of stage 2 (0, 20, 40, 80, 160, or 320 ms), two fixation period sequences (static followed by dynamic or vice versa), two speeds of motion, and two motion directions (leftward or rightward).

Results and discussion

Panels B to D of Figure 6 show the results of Experiment 4 for three subjects. Normalized OFR amplitudes are plotted. The OFRs were suppressed the most in the dynamic only condition (0 on the ordinate axis), whereas the static only condition was the one in which the suppression was minimal (1 on the ordinate axis). The OFR amplitudes transitioned smoothly between these two extreme values. Longer durations of dynamic stimulation immediately prior to motion stimulus produced stronger suppression. Longer durations of static stimulation prior to motion allowed for greater recovery from suppression. Both transitions were well fit (median $r^2 = 0.969$; range = 0.854–0.983) by exponential functions:

$$OFR = e^{-(T2-T0)/\tau}, \quad (5)$$

with T_0 (initial time integration period) and τ (time constant) as two free parameters. T2 is the stage 2 duration. The best-fit values of free parameters are listed in Table 2. In all three subjects, the suppression caused by stage 2 dynamic fixation pattern (solid-line fits) developed more quickly than the recovery from suppression (dashed-line fits) seen during stage 2 static stimulation. This was reflected in statistically significant differences in the time constant (τ) free parameter ($p < 0.01$; see Table 2).

Earlier studies reported a robust post-saccadic OFR enhancement in both human and non-human primate subjects (Gellman et al., 1990; Kawano & Miles, 1986). In monkeys, quite similar OFR enhancement was also observed in the wake of brief high-speed motion pulses applied to the visual scene, where as in humans such enhancement was minimal: up to 34% at 15 and 30 ms delays (which is the time interval between the end of a high-speed screen motion pulse and the start of the OFR-inducing motion stimulus), with no statistically significant enhancement at longer delays (up to 600 ms). As Gellman et al. (1990) put it: "In sum, visual enhancement in humans was very weak and transient, and could account for only a small part of the post-saccadic enhancement that we observed." In those earlier studies, the implemented speeds of motion of the visual scene were in the range of 100 to

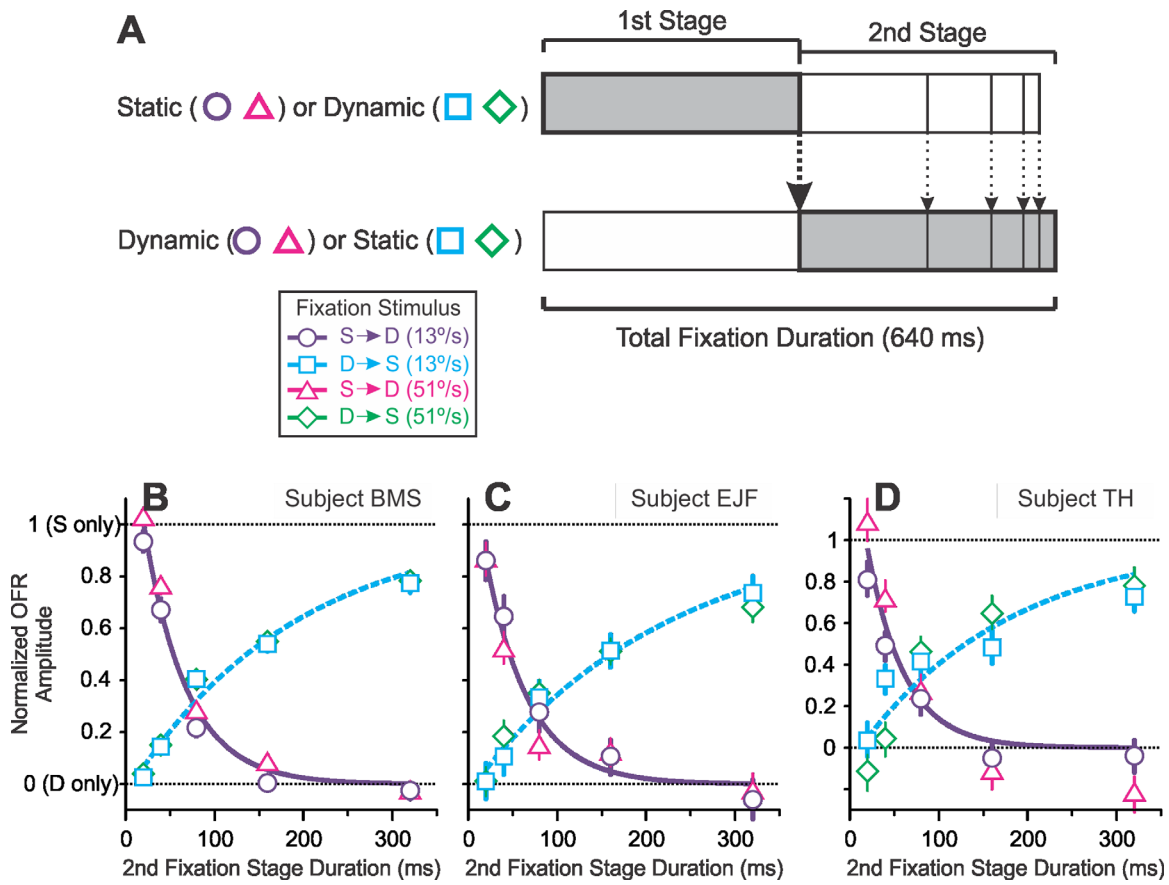

Figure 6. Experiment 4. (**A**) The time course of the fixation period of a single trial. The total duration was fixed at 640 ms and was subdivided into two stages, during which a static 1D vertical pink noise (S; static) was followed by a dynamic 1D vertical pink noise (D; dynamic) or vice versa: stages 1 and 2. In different conditions the duration of stage 2 was set to 0, 20, 40, 80, 160, or 320 ms. (**B–D**) OFR normalized amplitude dependencies to 1D vertical pink noise motion stimuli (13 degrees/s or 51 degrees/s) upon the second fixation stage duration (log abscissa). Symbols = data; solid smooth lines = exponential fits. Colored vertical lines = 68% confidence intervals of the mean (bootstrapping). (**B**) Subject BMS; (**C**) subject EJF; and (**D**) subject TH.

	Static → dynamic			Dynamic → static			Dy→St vs. St→Dy	
	T_0 (ms)	τ (ms)	r^2	T_0 (ms)	τ (ms)	r^2	T_0 (ms)	τ (ms)
BMS	20	48	0.983	8	185	0.974	$\mathbf{p < 0.01}$	$\mathbf{p < 0.01}$
EJF	13	49	0.971	7	221	0.966	$p = 0.62$	$\mathbf{p < 0.01}$
TH	18	42	0.918	12	171	0.854	$p = 0.50$	$\mathbf{p < 0.01}$

Table 2. Experiment 4: The best-fit values of free parameters for Equation 5.

600 degrees/s, and in monkeys the OFR were not much different at even 3000 degrees/s. Such regime of visual stimulation effectively amounted to "flicker," which, in principal, might be compared to our dynamic noise conditions (although in studies of Miles and colleagues it was a 2D one). In this vein, it was not surprising that Kawano and Miles did not find major differences in the magnitude of effects between opposite and same-direction conditioning ramps, because there is no such thing as "an opposite" or "same-direction" flicker.

An inspection of our Figures 6B to D of Experiment 4 reveals that in two subjects, (B) and (D), the OFRs in 20 ms S->D condition (i.e. when the static noise was replaced by a dynamic one just 20 ms before the motion stimulus was presented) were, on average, higher (i.e. enhancement) than the OFRs observed when the fixation pattern was static for the whole period. These effects were not significant, however. But again, Miles and colleagues' paradigms up to the moment of the motion stimulus presentation can be described as

static-dynamic-static, with the second "static" being a "delay," the duration of which they manipulated. In our Experiment 4, we do not have such a delay: motion stimulus follows dynamic noise right away. To sum, we feel that at present it is at least premature to try to draw parallels between our paper and those of Miles, et al. (1986) and Miles, et al. (1990).

General discussion

We find that the strength of OFR responses to moving stimuli is strongly dependent on the visual stimulus (the "fixation pattern") that precedes that motion. Most fixation patterns suppress OFRs (relative to a blank screen during fixation). This suppression contains a substantial component that depends on the spatiotemporal properties of the fixation pattern alone (independent of the moving pattern). There is also a substantial component that depends upon the relative orientation and spatial frequency of the two patterns. The time course of this suppression was asymmetric: it developed quickly, whereas the recovery was more gradual.

One natural way to express these results is in terms of adaptation – if the fixation patterns produce adaptation in channels that support the OFRs, it could produce many of these effects. Adaptation in direction selective channels is often studied psychophysically using the MAE. Studies of the MAE, which probed MAE spatial frequency (SF) tuning (e.g. Ashida & Osaka, 1994; Cameron, Baker, & Boulton, 1992; Ledgeway & Hutchinson, 2009; von Grunau & Dube, 1992) report strongest effects when the adapting and testing SFs are similar, although this correspondence does seem to break down under certain conditions (Ledgeway & Hutchinson, 2009; von Grunau & Dube, 1992). However, the traditional MAE paradigm involves much longer adaptation periods than the fixation period used in this study, so detailed comparisons may be hazardous. Furthermore, the adaptation period in our experiments used visual stimulation affecting the processing of stimuli of a much broader SF range. Thus, Experiment 2A used band-pass flicker fixation patterns. It was shown that a given motion stimulus produced a weaker OFR when combined with such flicker stimuli, and the strength of inhibition depended upon the flicker central SF (Sheliga et al., 2016). What it appears to suggest is that having a flicker as an adapting stimulus alters the responsiveness of neuronal circuits mediating the processing of stimuli of many different SFs, and the observed OFRs result from adaptive changes in many different SF channels. Fixation patterns in Experiment 2B were two same-central-SF band-pass motion stimuli moving in opposite directions. This arrangement might have led to shutting down this particular SF channel, which in turn could have shifted the balance of activation in circuits mediating the processing of other SFs during the adaptation period, and, as a result, the observed OFRs would again have been accounted for by the adaptive changes in many different SF channels. Fixation patterns in Experiment 3 were two band-pass motion stimuli of different central SF moving in opposite directions. It is well established that such stimulus configuration leads to an interaction between moving components (Kumbhani, Saber, Majaj, Tailby, & Movshon, 2008; Matsuura et al., 2008; Miura, Inaba, Aoki, & Kawano, 2014; Sheliga, FitzGibbon, & Miles, 2008; Sheliga et al., 2006; Sheliga et al., 2020). In the context of Experiment 3, one of them dominates the interaction, and its direction of motion gets suppressed (due to the requirement to maintain fixation), resulting in weaker OFRs to any subsequent motion stimulus in this direction.

The suppressive effects of dynamic fixation patterns reported in this paper were quite severe, and at this point one cannot rule out a possibility that some of the effects we report here are specific for the OFRs. However, our dynamic fixation stimuli were broadband and of high contrast, potentially affecting motion sensors tuned to a wide SF and directional selectivity range. Therefore, one might expect the effects to be stronger than, for example, those usually reported in pure sine wave studies (e.g. Kohn & Movshon, 2004; Nishida, Ledgeway, & Edwards, 1997). Hopefully, future work, both in psychophysics and electrophysiology, will help to develop a more complete picture.

Experiment 1 of this paper included the random-luminance blank screen condition (i.e. when the screen luminance was modulated [50 Hz] for the entire duration of the fixation period). We found that the OFRs were substantially weakened in this condition, showing that luminance manipulations affect responses to subsequently presented motion stimuli. In 1994, Kawano and colleagues compared the OFRs recorded in a traditional optokinetic setup—when a room, in which the experiments were run, was completely dark until the moment of motion stimulus presentation—with those recorded when there was no change in the overall luminance between the fixation and motion trial stages (Kawano, Shidara, Watanabe, & Yamane, 1994). A 35 to 40 ms delay in the OFR onset in the "optokinetic" condition was observed. Macaque monkeys were subjects in that study, so neuronal recordings were also performed in area MST, known to be crucial for the OFR production (Takemura, Murata, Kawano, & Miles, 2007). Kawano et al. (1994) were able to show that motion-related neuronal activation in area MST in the optokinetic setup was also delayed and preceded by a transient on-response, related to an abrupt change in luminance, but not to motion stimulus per se. Qualitatively similar phenomena were also observed in human subjects: in one of the conditions in a study conducted by Taki et al. (2009), a motion stimulus appeared after a brief period of darkness,

and the associated OFRs were severely attenuated. So, it is plausible to suggest that weaker OFRs in random-luminance blank screen condition of our current study could be accounted for by the repetitive ON- and OFF-responses arising from the earliest stages of visual processing—evoked due to dynamic temporal structure of our fixation stimulus—which impeded the responses to motion per se.

Keywords: visual motion, spatial frequency tuning, spatially non-oriented and oriented inhibition

Acknowledgments

Supported by the Intramural Program of the National Eye Institute at the National Institutes of Health (NIH).

Commercial relationships: none.
Corresponding author: Boris M. Sheliga.
Email: bms@lsr.nei.nih.gov.
Address: Laboratory of Sensorimotor Research, National Institutes of Health Building 49 Room 2A50, 49 Convent Drive, Bethesda, MD 20892-4435, USA.

Footnotes

[1]Subjects EJF and TH ran fewer conditions, see Figure 2.
[2]Subjects EJF and TH ran fewer conditions, see Figure 2.
[3]OFRs recorded with dynamic fixation patterns of the highest central SF (2 and 2.93 cpd) in subject TH were the only exception.

References

Ashida, H., & Osaka, N. (1994). Difference of spatial frequency selectivity between static and flicker motion aftereffects. *Perception, 23*(11), 1313–1320.

Brainard, D. H. (1997). The Psychophysics Toolbox. *Spatial Vision, 10*(4), 433–436.

Burr, D., & Thompson, P. (2011). Motion psychophysics: 1985-2010. *Vision Research, 51*(13), 1431–1456.

Cameron, E. L., Baker, C. L., Jr., & Boulton, J. C. (1992). Spatial frequency selective mechanisms underlying the motion aftereffect. *Vision Research, 32*(3), 561–568.

Collewijn, H., Van Der Mark, F., & Jansen, T. C. (1975). Precise recording of human eye movements. *Vision Research, 15*, 447–450.

De Valois, R. L., Albrecht, D. G., & Thorell, L. G. (1982). Spatial frequency selectivity of cells in macaque visual cortex. *Vision Research, 22*(5), 545–559.

Gellman, R. S., Carl, J. R., & Miles, F. A. (1990). Short latency ocular-following responses in man. *Visual Neuroscience, 5*(2), 107–122.

Hays, A. V., Richmond, B. J., & Optican, L. M. (1982). A UNIX-based multiple process system for real-time data acquisition and control. *WESCON Conference Proceedings, 2*(1), 1–10.

Hutchinson, C. V., & Ledgeway, T. (2007). Asymmetric spatial frequency tuning of motion mechanisms in human vision revealed by masking. *Investigative Ophthalmology & Visual Science, 48*(8), 3897–3904.

Kawano, K., & Miles, F. A. (1986). Short-latency ocular following responses of monkey. II. Dependence on a prior saccadic eye movement. *Journal of Neurophysiology, 56*(5), 1355–1380.

Kawano, K., Shidara, M., Watanabe, Y., & Yamane, S. (1994). Neural activity in cortical area MST of alert monkey during ocular following responses. *Journal of Neurophysiology, 71*(6), 2305–2324.

Kohn, A., & Movshon, J. A. (2004). Adaptation changes the direction tuning of macaque MT neurons. *Nature Neuroscience, 7*(7), 764–772.

Krekelberg, B., van Wezel, R. J., & Albright, T. D. (2006). Adaptation in macaque MT reduces perceived speed and improves speed discrimination. *Journal of Neurophysiology, 95*(1), 255–270.

Kumbhani, R. D., Saber, G. T., Majaj, N. J., Tailby, C., & Movshon, J. A. (2008). *Contrast affects pattern direction selectivity in macaque MT neurons*. *Program No. 460.26*, 2008 Neuroscience Meeting Planner. Washington, DC: Society for Neuroscience, 2008. Online.

Ledgeway, T., & Hutchinson, C. V. (2009). Visual adaptation reveals asymmetric spatial frequency tuning for motion. *Journal of Vision, 9*(1), 4 1–9.

Masson, G. S., & Perrinet, L. U. (2012). The behavioral receptive field underlying motion integration for primate tracking eye movements. *Neuroscience and Biobehavioral Reviews, 36*, 1–25.

Mather, G., Pavan, A., Campana, G., & Casco, C. (2008). The motion aftereffect reloaded. *Trends in Cognitive Science, 12*(12), 481–487.

Matsuura, K., Miura, K., Taki, M., Tabata, H., Inaba, N., & Kawano, K. et al. (2008). Ocular following responses of monkeys to the competing motions of two sinusoidal gratings. *Neuroscience Research, 61*(1), 56–69.

Miles, F. A. (1998). The neural processing of 3-D visual information: evidence from eye movements. *The European Journal of Neuroscience, 10*(3), 811–822.

Miles, F. A., Kawano, K., & Optican, L. M. (1986). Short-latency ocular following responses of monkey. I. Dependence on temporospatial properties of

visual input. *Journal of Neurophysiology, 56*(5), 1321–1354.

Miles, F. A., & Sheliga, B. M. (2010). Motion detection for reflexive tracking. In U. Ilg, & G. S. Masson (Eds.), *Dynamics of Visual Motion Processing: Neuronal, Behavioral and Computational Approaches* (pp. 141–160). New York, NY: Springer-Verlag.

Miura, K., Inaba, N., Aoki, Y., & Kawano, K. (2014). *Responses of MT/MST neurons elicited by dual-grating stimulus: Differences between areas MT and MST*. Program No. 726.709. 2014 Neuroscience Meeting Planner. Washington, DC: Society for Neuroscience, 2014. Online.

Nishida, S., Ledgeway, T., & Edwards, M. (1997). Dual multiple-scale processing for motion in the human visual system. *Vision Research, 37*(19), 2685–2698.

Pantle, A. (1971). Flicker adaptation. I. Effect on visual sensitivity to temporal fluctuations of light intensity. *Vision Research, 11*(9), 943–952.

Pelli, D. G. (1997). The VideoToolbox software for visual psychophysics: transforming numbers into movies. *Spatial Vision, 10*(4), 437–442.

Priebe, N. J., & Lisberger, S. G. (2002). Constraints on the source of short-term motion adaptation in macaque area MT. II. tuning of neural circuit mechanisms. *Journal of Neurophysiology, 88*(1), 370–382.

Robinson, D. A. (1963). A method of measuring eye movement using a scleral search coil in a magnetic field. *Institute of Electronic and Electrical Engineers: Transactions in Biomedical Engineering, BME-10*, 137–145.

Sheliga, B. M., Chen, K. J., FitzGibbon, E. J., & Miles, F. A. (2005). Initial ocular following in humans: a response to first-order motion energy. *Vision Research, 45*, 3307–3321.

Sheliga, B. M., FitzGibbon, E. J., & Miles, F. A. (2008). Human ocular following: evidence that responses to large-field stimuli are limited by local and global inhibitory influences. *Progress in Brain Research, 171*, 237–243.

Sheliga, B. M., Kodaka, Y., FitzGibbon, E. J., & Miles, F. A. (2006). Human ocular following initiated by competing image motions: evidence for a winner-take-all mechanism. *Vision Research, 46*(13), 2041–2060.

Sheliga, B. M., Quaia, C., Cumming, B. G., & Fitzgibbon, E. J. (2012). Spatial summation properties of the human ocular following response (OFR): dependence upon the spatial frequency of the stimulus. *Vision Research, 68*, 1–13.

Sheliga, B. M., Quaia, C., FitzGibbon, E. J., & Cumming, B. G. (2016). Ocular-following responses to white noise stimuli in humans reveal a novel nonlinearity that results from temporal sampling. *Journal of Vision, 16*(1), 8.

Sheliga, B. M., Quaia, C., FitzGibbon, E. J., & Cumming, B. G. (2017). *Short-latency ocular responses are strongly affected by the visual content during the initial fixation period directions*. *Program No. 685.10*, 2017 Neuroscience Meeting Planner. Washington, DC: Society for Neuroscience, 2017. Online.

Sheliga, B. M., Quaia, C., FitzGibbon, E. J., & Cumming, B. G. (2018). Short-latency ocular-following responses to motion stimuli are strongly affected by temporal modulations of the visual content during the initial fixation period. *Journal of Vision, 18*(10), 351.

Sheliga, B. M., Quaia, C., FitzGibbon, E. J., & Cumming, B. G. (2020). Short-latency ocular-following responses: Weighted nonlinear summation predicts the outcome of a competition between two sine wave gratings moving in opposite directions. *Journal of Vision, 20*(1), 1.

Smith, R. A., Jr. (1970). Adaptation of visual contrast sensitivity to specific temporal frequencies. *Vision Research, 10*(3), 275–279.

Solomon, S. G., & Kohn, A. (2014). Moving sensory adaptation beyond suppressive effects in single neurons. *Current Biology: CB, 24*(20), R1012–R1022.

Takemura, A., Murata, Y., Kawano, K., & Miles, F. A. (2007). Deficits in short-latency tracking eye movements after chemical lesions in monkey cortical areas MT and MST. *The Journal of Neuroscience, 27*(3), 529–541.

Taki, M., Miura, K., Tabata, H., Hisa, Y., & Kawano, K. (2009). The effects of prolonged viewing of motion on short-latency ocular following responses. *Experimental Brain Research, 195*(2), 195–205.

von Grunau, M., & Dube, S. (1992). Comparing local and remote motion aftereffects. *Spatial Vision, 6*(4), 303–314.

Yang, D. S., FitzGibbon, E. J., & Miles, F. A. (2003). Short-latency disparity-vergence eye movements in humans: sensitivity to simulated orthogonal tropias. *Vision Research, 43*(4), 431–443.

Yang, J., & Lisberger, S. G. (2009). Relationship between adapted neural population responses in MT and motion adaptation in speed and direction of smooth-pursuit eye movements. *Journal of Neurophysiology, 101*(5), 2693–2707.